Konya Mühendislik Bilimleri Dergisi, c. 9, s. 1, 124-139, 2021
Konya Journal of Engineering Sciences, v. 9, n. 1, 124-139, 2021
ISSN: 2667-8055 (Elektronic)
DOI: 10.36306/konjes.767269

FABRICATION OF UNDERCOOLED BISMUTH TIN LIQUID METAL PARTICLES WITH HIGH YIELD

Simge ÇINAR

[1] *Middle East Technical University, Department of Metallurgical and Materials Engineering, Ankara, TURKEY*
csimge@metu.edu.tr

(Geliş/Received: 09.07.2020; Kabul/Accepted in Revised Form: 28.10.2020)

ABSTRACT: Despite increasing attention to the liquid metals, most of the studies in this field have focused on the gallium-based alloys due to their low melting points. The examples of metastable undercooled liquid metal particles are rare due to the thermodynamic challenges in achieving significant level of undercooling. In this study, the fabrication of undercooled bismuth-tin (BiSn) liquid metal micro-/nano-particles at eutectic composition was studied. The droplet emulsion technique was used for particle formation in broad size range. The effects of the particle size and the shell formation reactions on the yield of undercooled particles were investigated. The fabricated particles were characterized using back-scattered scanning electron microscopy (BSE-SEM) and differential scanning calorimetry (DSC). The particle size distribution and the ratio of undercooled particles were statistically analyzed. Optimization of the processing conditions and the successful selection of oxidants enabled undercooling of BiSn liquid metal particles. In doing so, both micro- and nano-size particles could be fabricated with high yield (≥ 97%). The crystallization temperature was measured to be 0.37 T_m and the particles could preserve their liquid state at room temperatures for months.

Key Words: *Liquid metals, bismuth-tin particles, undercooled particles, droplet emulsion technique, yield of undercooled particles*

Aşırı Soğumuş Bizmut Kalay Sıvı Metal Parçacıklarının Yüksek Verimle Üretimi

ÖZ: Sıvı metallere artan ilgiye rağmen, bu alandaki çalışmaların çoğu düşük erime noktaları nedeniyle galyum bazlı alaşımlara odaklanmıştır. Yarı-kararlı aşırı-soğumuş sıvı metal parçacık örnekleri yüksek seviyelerde aşırı-soğuma elde edilmesindeki termodinamik zorluklardan ötürü oldukça nadirdir. Bu çalışmada, ötektik kompozisyonda aşırı-soğumuş bizmut kalay (BiSn) sıvı metal mikron/nano parçacıklarının üretimi incelenmiştir. Geniş boyut aralığında parçacık üretimi için damlacık emülsiyon tekniği kullanılmıştır. Parçacık boyutu ve kılıf oluşum tepkimelerinin aşırı-soğumuş parçacık verimi üzerindeki etkileri araştırılmıştır. Üretilen parçacıklar geri saçılımlı taramalı elektron mikroskobu (BSE-SEM) ve diferansiyel taramalı kalorimetri (DSC) kullanılarak analiz edilmiştir. Parçacık boyut dağılımı ve aşırı-soğumuş parçacık oranı istatistiksel olarak karakterize edilmiştir. Üretim koşullarının optimizasyonu ve başarılı oksidan seçimi BiSn sıvı metal parçacıklarının aşırı-soğutulmasını sağladı. Bunu yaparken hem mikro hem de nano boyutlu parçacıklar yüksek verimle (≥ 97%) üretilebildi. Kristalleşme sıcaklığı 0.37 T_e olarak ölçüldü ve parçacıklar sıvı hallerini oda sıcaklığında aylarca koruyabildiler.

Anahtar Kelimeler: *Sıvı metaller, bizmut-kalay parçacıkları, aşırı-soğumuş parçacıklar, damlacık emülsiyon tekniği, aşırı-soğumuş parçacıkların verimi*

1. INTRODUCTION

Liquid metals are emerging class of materials with an enormous potential in the research fields of physical chemistry, material synthesis, composites, electronics, energy, nanotechnology and biotechnology (Wang *et al.,* 2018a; Chen *et al.,* 2020; Daeneke *et al.,* 2018; Mahmood *et al.,* 2019; Kalantar-Zadeh *et al.,* 2019; Malakooti *et al.,* 2020; Yuan *et al.,* 2020; Wang and Liu 2013; Xu *et al.,* 2020). Liquid metals owe this interest mainly to their extraordinary properties stemming from being both metallic and liquid. Being flexible and electrically conductive enables their use in flexible composites, transient and self-healing electronics, microfluidic chips and robotics (Wang *et al.,* 2018b; Silva *et al.,* 2020; Idrus-Saidi *et al.,* 2020; Chang *et al.,* 2018; Kalantar-Zadeh *et al.,* 2019). Due to their ability to respond to external stimuli such as light, pH, chemicals, and/or temperature, they can be applied to theranostics, sensors, batteries and conductor–insulator transition materials (Idrus-Saidi *et al.,* 2020; Ding *et al.,* 2020). Moreover, liquid metals are commonly covered by native, self-limiting oxide layers which are almost atomically thin, therefore liquid metals have been used as a platform to fabricate low dimensional materials (Idrus-Saidi *et al.,* 2020; Wang and Liu 2013; Yuan *et al.,* 2020; Li *et al.,* 2020; Mahmood *et al.,* 2019). Utilizing the flexibility of a liquid metal core, these ultrathin materials can find applications in heterostructured optoelectronics, photodetectors, catalysis, and energy storage. Even though liquid metals can be present in both bulk or particle forms; due to the high surface to volume ratio, particle form is commonly preferred and the fabrication of liquid metal micro or nanoparticles become a crucial step to realize many of the aforementioned applications.

Liquid metals are commonly defined as the metals that are liquid at temperatures below 300 °C (Kalantar-Zadeh *et al.,* 2019). Even though the liquid metal particles can be used at broad temperature ranges, the ones that are liquid around room temperature have attracted significant attention due to the wider possibilities of potential applications. Daeneke *et al.* listed the metals and alloys that are commonly known with low melting points. (Daeneke *et al.,* 2018) In this list, mercury is liquid at room temperature, but its use is avoided due to health concerns. Gallium and its alloys remain as the only metal group which are liquid around room temperature under equilibrium conditions and that is why the current studies on liquid metals are commonly focused on, but also limited to the Ga-based materials (Kalantar-Zadeh *et al.,* 2019; Lin *et al.*, 2020).

To extend the material portfolio for room temperature-liquid metals, metastable metallic particles, particularly undercooled (a.k.a. supercooled) particles, are a promising option, but their current examples are rare mostly because of the thermodynamic constraints (Kalantar-Zadeh *et al.,* 2019). One example of metastable liquid metals reported in the literature is the undercooled Field's metal (a eutectic alloy composed of bismuth, indium and tin). Even though the equilibrium melting point of Field's metal is 62 °C, its solidification could be retarded down to the temperatures below the room temperature by optimizing its core-shell structure, therefore it became possible to store Field's metal in its liquid state at room temperatures. In this study, the shell structure around Bi-In-Sn particles was obtained by fabrication of Field's metal particles in slightly acidic media obtained using acetic acid. Manipulation of crystallization process allowed the use of such particles to form complex three-dimensional structures (Çınar *et al.,* 2016; Martin *et al.,* 2019) and as heat-free micro- or nano-solders (Çınar *et al.,* 2016; Qu *et al.,* 2015). Bismuth-tin at eutectic composition is another example of room temperature undercooled alloy reported in the same study, yet it has not been demonstrated in any application. That is probably because of its low yield of undercooling, which is the number of undercooled particles with respect to the solid particles prepared in the same batch, to enable any feasible application.

The equilibrium melting temperature for the bismuth-tin system at the eutectic composition is 139 °C (Şekil 5b), that is much higher compared to that of Field's metal. Since the driving force of crystallization is increasing significantly as getting far from the equilibrium conditions, it is even more challenging to keep undercooled bismuth tin (BiSn) at this metastable state long enough to enable any application. However, if it can be achieved, it will not only make the applications of liquid BiSn micro-/nano-particles possible at room temperatures, but also will pave way for the fabrication of other metastable liquid metals

with relatively high melting points and extend the liquid metal particle portfolio. Moreover, undercooled particles may offer far-from-equilibrium properties, thus may enable many unprecedented applications. In this study, with this motivation, we aimed to investigate the effect of shell formation on the fabrication and undercooling of BiSn micro-/nano-particles. With this, we also focused on fabricating undercooled BiSn micro-/nano-particles with high yield, thus enable its use as the room-temperature liquid metal alloy. BiSn particles can be a strong material candidate in this field, because the eutectic BiSn is one of the alloys having higher melting point than Fields metal and lower melting point than many other low temperature alloys. Moreover, its superior properties have received increased attention to in recent years and found use as energy materials (Wang and Liu 2013; Niu *et al.,* 2018; Niu *et al.,* 2019), catalyst (Allioux *et al.,* 2020), lead-free solder (Firdaus *et al.,* 2020; Felton *et al.,* 1993; Kang and Sarkhel, 1994), X-Ray radiation shield (Kim *et al.,* 2020).

Undercooling (a.k.a. supercooling) phenomenon plays critical role in the solidification process and directly affects the microstructure, hence the material properties, of an alloy, therefore it has attracted significant attention in the recent literature (Thompson and Spaepen 1983; Greer 2010; Liu *et al.,* 2019; Zahir *et al.,* 2019; Schülli *et al.,* 2010; Herlach 1991). Droplet emulsion technique (DET) is commonly used to prepare undercooled liquid metal droplets in large scale (Herlach *et al.,* 1993). In DET, metal/alloy melt is separated into smaller units using high speed stirring in a carrier fluid which is slightly oxidizing (Rasmussen and Loper 1975; Herlach *et al.,* 1993). In this process, high speed stirring provides the energy to break the metal droplets into smaller pieces and to create new surfaces. Because of the oxidative environment of the reaction media, which is commonly a slightly acidic environment, a very thin surface layer is formed around each particle during stirring, and this oxide encapsulation protects the particles from re-coalescence even after the stirring process. During the droplet emulsion process, among all the fabricated particles, the impurities act as catalytic nucleation sites for crystallization, and are enclosed in a small fraction of the particles. The remaining particles become free from internal nuclei and surface nucleation sites, the crystallization mechanism switches from the heterogeneous nucleation toward the homogeneous nucleation, therefore the particles undercool due to the retardation of crystallization to the temperatures lower than the equilibrium solidification temperature of the metal.

DET results in particles with diameters around 10 – 20 μm and allows to achieve the undercooling range around 0.3 – 0.4 T_m (Perepezko 1984; Herlach *et al.,* 1993). In order to obtain such a high undercooling ($\Delta T = T_m - T_c$, where T_m is the equilibrium melting point and T_c is the crystallization temperature of undercooled particles), a number of processing parameters including size refinement and powder surface coating, have been experimentally identified. It has been reported that as the particle size gets smaller, the possibility for heterogeneous nucleation will be lower, thus the level of undercooling will be higher (Perepezko and Wilde 2016; Herlach 1991). At the same time, since the possibility of impurity being in one particle will be less, the fraction of undercooled particles in a batch, i.e. the yield of undercooling, will increase. As cooling gets faster, which is also the case in particles with smaller size, the particles tend to undercool more (Perepezko and Paik 1981; Zhai *et al.,* 2006). The formation of the protective layer is still a key challenge in fabrication of liquid micro- or nano- particles (Daeneke *et al.,* 2018; Kalantar-Zadeh *et al.,* 2019), and it is even more critical for fabrication of undercooled particles (Bogatyrenko *et al.,* 2018; Çınar *et al.,* 2016; Perepezko and Wilde 2016; Perepezko and Paik 1981; Rasmussen and Loper 1975). The protective shell layer encapsulating the internal nuclei-free metals/alloys should be design in such a way that it should be almost perfectly smooth to eliminate any potent nucleation points, and should be thick, thus strong and/or flexible, enough to be mechanically stable, but should not be too thick to prevent initiation of nucleation on oxide walls. Droplet undercooling behavior can be controlled by size variation, but the achievable level of undercooling is often set by the surface coating, which is consistent with the classical nucleation theory (Perepezko, 1984). Therefore, the design of the particle shell is vital for fabrication of undercooled particles with high yield.

There are two common approaches to form protective shell layer for stabilization of liquid droplets: formation of a self-limiting oxide layer and utilization of ligands adsorbing on the surface of liquid metal particles. The properties of the protective layer and interactions between the substrate (the power coating)

and the metal melt governs the possibility and the state of undercooling. In the literature, to best of our knowledge, there is only one study reporting the formation of BiSn liquid metal particles by DET and 1 vol% of acetic acid in diethylene glycol was used as a reaction media (Çınar *et al.,* 2016). There are few other examples where BiSn particles were fabricated via similar techniques but under different conditions. While Gong *et al.* (2020) used high speed stirring of bismuth-tin alloy melt in paraffin and polyethylene glycol and produced particles with sizes in the range of 1.9 – 27.6 μm, Allioux *et al.* (2020) sonicated BiSn alloy melt in glycerol with sodium bicarbonate and fabricated particles having diameters of 8.5 ± 4.8 μm. Similarly, Kang *et al.* (2019) used ultrasonication in a silicon oil and controlled the mean particle size between 92 to 506 nm by variations in ultrasonication power and irradiation time. However, in all of these studies, the resulting particles were completely solid.

In this study, we hypothesized that undercooled particles can be fabricated with high yield by control over the particle size and the surface coating. To this end, in this study, we investigate effects of the oxidant type, the oxidant concentration, and stirring duration to fabricate undercooled BiSn micro-/nano-particles with varying particle size. The effect of surface coating on the particle formation and the yield of undercooled particles were discussed. Acetic acid and oxygen are evaluated as oxidants for fabrication of BiSn liquid metals with high yield.

2. MATERIALS AND METHODS

2.1. Materials

Bismuth-tin alloy at eutectic composition (Bi:Sn 58:42 wt%, purity ≥ 99.9%, m. p. ≈ 138 °C), acetic acid (glacial, ≈100%) and diethylene glycol (ReagentPlus, 99%) were purchased from Rotometals, Merck and Sigma Aldrich, respectively. Technical grade ethanol was used for cleaning and storage.

2.2. Particle fabrication procedure

In order to prepare the set up for particle preparation, a glass vial (volume ≈ 25 ml) was placed in a silicon oil bath. For stirring, a cross-shaped poly(tetrafluoroethylene) rod was implemented to a dremel tool (Dremel 4000) and it was placed as close as possible to vial wall to enhance the effect of shear in a glass vial. Stirring rate was measured using digital tachometer. The highest stirring rate that could be achieved at the highest power settings of the Dremel tool was recorded as 12,000 ± 1,000 rpm and this rate was kept constant for all experiments in order to favor smaller particle formation.

Diethylene glycol was used as a carrier fluid because of its relatively high boiling point and inert nature towards BiSn alloy. In order to fabricate liquid BiSn metal particles, 10 ml of diethylene glycol was heated to 160 ± 5 °C (≈ T_m + 20 °C) in a glass vial. Then a piece of BiSn alloy at eutectic composition (1.0 ± 0.1 g) was added into diethylene glycol and let to melt for 1 min. Acetic acid, if used, was added afterwards, and the solution was stirred at a rate of 12,000 ± 1,000 rpm to form micro/nano-droplets. When used, the concentration of the acetic acid was calculated as a volume percentage of the diethylene glycol. For 0.25 vol% acetic acid experiments, for example, 25 μl of acetic acid was used. Depending on the experiments, three different acetic acid concentrations, 0.25 vol%, 1 vol% and 2 vol%, were used. The time started to be recorded once stirring started. After couple of minutes, the color of the solution started to turn gray indicating the formation of particles. At the end of the stirring process, the glass vial was taken out of the oil bath and the particles were washed with ethanol via centrifugation at 5,000 rpm for 15 min. The washing procedure was repeated twice in order to clean the remaining organics on particle surfaces. After the washing procedure, the BiSn particles were stored in ethanol.

2.3. Characterization of particles

For SEM analysis, the particles in ethanol were dropped onto a silicon wafer and left for drying prior to analysis and the back-scattered scanning electron microscopy (BSE-SEM, Nova, NanoSEM 430) was used.

For the statistical analysis of the solid and undercooled particles, at least 400 particles were analyzed using BSE-SEM micrographs, and measurements were conducted manually using ImageJ software. Number percentage of both solid and undercooled particles as well as the cumulative size distribution of the total number of particles were presented.

For differential scanning calorimetry (DSC, Hitachi, EXSTAR7000) experiments, aluminum pan and lids were used. The particles were dropped into pan and left for drying overnight. About 1 mg of particles were collected in a pan. The sample was first cooled from 30 °C to -80 °C with cooling rate of 5 °C /min, left at this temperature for 2 min to equilibrate, then heated back to 30 °C with the same rate.

2.4. BiSn phase diagram

The phase diagram of Bi-Sn system was calculated under 1 atm pressure and in the range of 50 - 300 °C using Thermo-calc software. The alpha-tin phase, the transformation which occurs at 13°C, was disabled during calculations because the transformation is not observed experimentally in BiSn alloys of eutectic composition.

3. RESULTS AND DISCUSSION

3.1. Fabrication of BiSn particles using acetic acid

BiSn particles fabricated using 0.25 vol% acetic acid by stirring for 10 min were presented in Figure 1a and 1b. As shown in Figure 1a-c, spherical particles with smooth surfaces were successfully fabricated and have a broad size distribution ranging from hundred nanometers to few tens of micrometers. Compared to the literature values where the fabrication of micron-sized particles was commonly reported for droplet emulsion technique, the formation of particles in nanometer size range is noteworthy.

In eutectic alloys, components are completely soluble in the liquid state, but only partially soluble in the solid state. These insoluble phases form a characteristic lamellar microstructure. In BSE-SEM micrographs, bismuth-rich phases seem brighter compared to tin-rich phases because of bismuth's higher atomic number. As realized in Figures 1a, 1b and 1c, both unicolor and bicolor particles existed in the sample. Bicolor of particles is a clear indication of a solid alloy. Presence of unicolor particles, on the other hand, indicates complete solubility, which is the case in liquid state at eutectic composition. Similar observations were reported previously for undercooled alloys and verified with complementary techniques (Çınar *et al.*, 2016). Therefore, as observed in Figures 1a-c, both solid and undercooled particles could be produced at the reported conditions. Even though smaller particles tend to be undercooled more, it was evident from the micrographs that undercooled particles as large as 15 μm can also be fabricated. Moreover, considering that the particles were stored and analyzed at room temperature, they are undercooled more than 100 degrees (melting point of eutectic BiSn is 138.4 °C, Figure 5). According to the statistical analysis of fabricated particles, presented in Figure 1d, 80% of the fabricated particles were undercooled, and the average particle size (D_{50}) of the fabricated undercooled particles were 1.7 μm while 90% of them have diameter were below 4 μm, i.e. D_{90} = 4 μm. In order to obtain a batch of undercooled particles with high yield, the particles can be separated by their size. As an example, if the particles with a diameter of 2 μm or less were separated, then the yield of undercooling would be around 99%.

Even though the number of fabricated undercooled particles are significantly high in this experiment, since the solid particles are larger in size, the weight percentage of the undercooled materials can be considered low. It is known that the droplet emulsion technique leads to the formation of undercooled particles by retarding the nucleation event, i.e. heterogenous nucleation. That happens because the

heterogeneous nucleation sites for solidification are eliminated by trapping the impurities in few fractions of fabricated particles, and the container effects are minimized and the system is pushed towards containerless solidification. Since homogeneous nucleation requires very high driving force for solidification, the particles can be undercooled to the temperatures way below their equilibrium melting points. Therefore, if the average particle size of the particles can be reduced, then the impurities will be trapped in fewer percentage of particles, therefore the overall yield of undercooling can be improved.

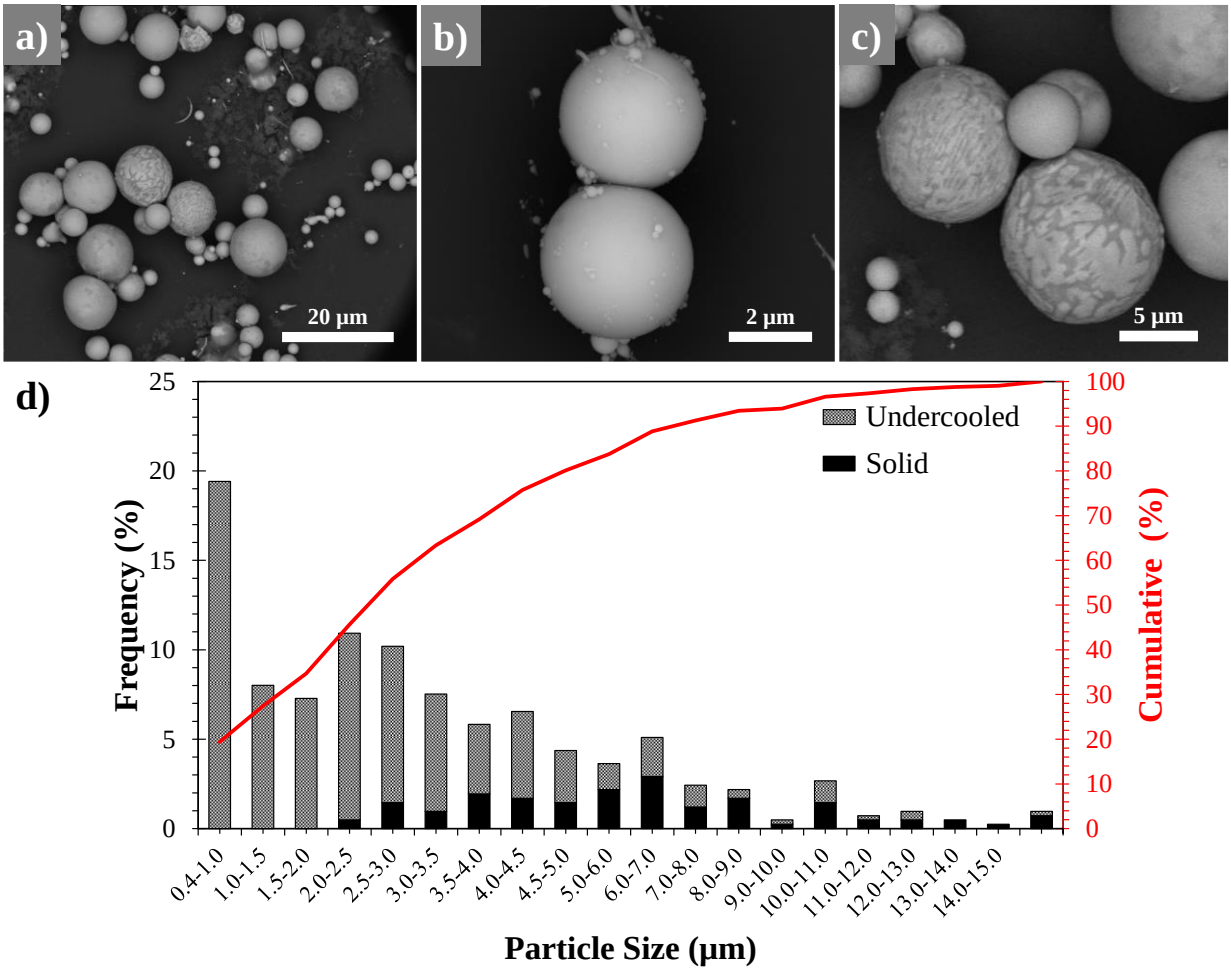

Figure 1. BSE-SEM characterization of fabricated BiSn particles. 0.25 vol% acetic acid used, and a metal melt was stirred for 10 min. In (a), both solid and undercooled particles can be observed. In (b) and (c) undercooled and solid particles were presented in larger magnifications, respectively. In (d) the frequency and cumulative size distributions of the fabricated particles and contribution of the solid and undercooled particles to the size distribution were presented.

3.2. Effect of stirring duration on the production efficiency of undercooled BiSn particles

In order to decrease the average particle size of the particles, either higher stirring rates or longer stirring durations may be employed. In order to get benefit from the size effect on the undercooled particle yield, the stirring duration was altered. It was first increased from 10 min to 30 min under the same experimental conditions. As a result, the particles with spherical shape and smooth surfaces could still be obtained as shown in BSE-SEM micrographs in Figures 2a and 2b. However, the statistical analysis of the particles presented in Figure 2c showed that the number of solid particles were increased unexpectedly

under these experimental conditions. 85% of the fabricated particles were solid. Moreover, the average particle size was increased rather than decreased. The average particle size (D_{50}) was found to be 6.8 µm. The significant portion of the fabricated undercooled particles were only about 500 nm in size. It was realized that a piece of metal about few millimeters in size was formed during this experiment. This metal piece was analyzed using BSE-SEM (Figure 3a), and it was revealed that its surface was almost pure bismuth with inclusions of tin. The chemical content of the particles fabricated from the same batch was analyzed using EDS and found that they were still at eutectic composition.

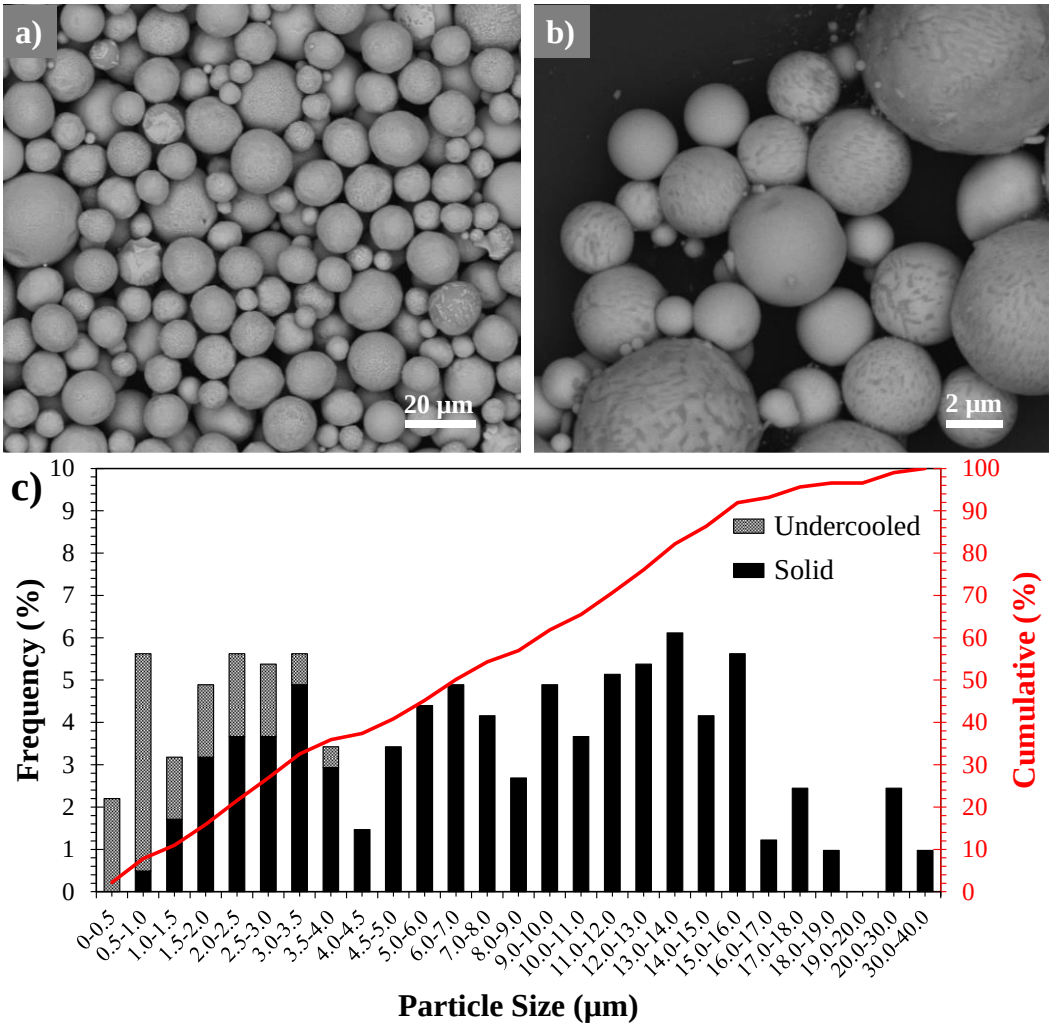

Figure 2. BSE-SEM characterization of BiSn particles fabricated by use of 0.25 vol% acetic acid and stirring for 30 min. Average particles size can be conceived in (a) and undercooled particles can be distinguished in (b). (c) shows the particle size distribution of the fabricated undercooled, solid and total number of particles.

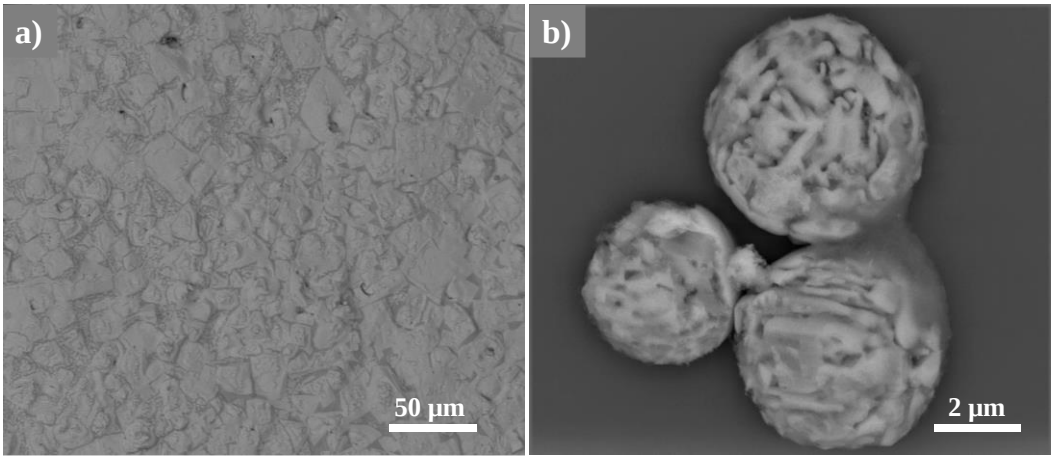

Figure 3. BSE-SEM images of the large metal piece formed during/after the experiments conducted using acetic acid of 0.25 vol% and stirred for 30 min (a); and using acetic acid of 2 vol% and stirred for 10 min (b).

3.3. Effect of acetic acid concentration on the production efficiency of undercooled BiSn particles

It is known that tin is more reactive in acidic conditions when compared to bismuth. In order to investigate the relation between the acetic acid concentration and the particle formation, acetic acid concentration was increased from 0.25 vol% to 1 vol% and 2 vol%, respectively, and the particle formation procedure was repeated for 10 min. In each case, formation of a millimeter-range solid metal piece was observed, and their BSE-SEM micrographs were almost identical to the one presented in Figure 3a. The concentration at which the highest number of particles were fabricated was 0.25 vol%. The particles could still be produced when the acetic acid concentration was 1 vol%. When the acid concentration was increased to 2 vol%, the color of the solution was dark grey at the beginning as usual, but then slightly turned to white. At the end of the particle formation procedure, very few particles could be formed. As shown in Figure 3b, those particles were still spherical but the tin content in particles was almost completely etched out. The gray cloud around particles in Figure 3-b was also an indication of the etched tin and it potentially oxidized and/or formed complexes with acetic acid (Chang *et al.*, 2019; Çınar *et al.*, 2016).

In the undercooled particle formation process suggested here, first, the small particles are separated from the metal melt once the Rayleigh-Plateau limit is reached (Tevis *et al.*, 2014), then with the effect of shear forces, spherical particles are formed. In the media containing oxidants, the particle surfaces are coated with a thin layer of metal-oxide or organic molecule-metal oxide complexes. Particularly at the very first stage of the particle formation process, these layers are hypothesized be too thin to protect the particles, and will either be broken into smaller pieces with an effect of stirring process or dissolve in relatively acidic reaction media. As stirring continues with the effects of extended time and applied shear force, the particles will get smaller and stronger surface layers may start to form. In order to form a good surface layer, thus enable the formation of spherical undercooled BiSn liquid metal particles with high yield, under these conditions, the oxide formation and dissolution reactions should reach an equilibrium. If the dissolution reaction dominates over the oxidation reactions, excessive dissolution of Sn does not allow the formation of a protective layer and may result in the formation of a hyper-eutectic (bismuth-rich) alloy (Figure S1). In the absence of the protective layer, these bismuth-rich metal droplets would coalesce back and form large metal pieces. At even more extreme conditions, the alloy composition may change so drastically that the melting point of alloy may shift to the higher temperatures (Figure 5), and the alloy tends to solidify at reaction temperature (~ 160 °C). The dissolution reaction may continue after solidification. Bismuth-rich composition of the large metal piece observed after the experiment (Figure 3a) and excessive dissolution of Sn in the particle form (Figure 3b) are evidences of this hypothesis. It can be

concluded that the optimization of shell formation, i.e. oxidation and dissolution, reactions are extremely critical to fabricate undercooled liquid metal micro-/nano-particles with high yield.

3.4. Native oxide layer as a shell and its effect on the fabrication of undercooled BiSn particles

Based on our observations in the previous experiments, in order to favor the fabrication of undercooled BiSn particles, mild reaction conditions should be preferred. It is known that tin forms a very thin protective oxide layer when BiSn alloy is exposed to ambient atmosphere (Frongia *et al.*, 2015; Allioux *et al.*, 2020). In order to create milder reaction conditions, bismuth-tin particles were prepared under similar conditions without any addition of external oxidizing agents, but by relying on the oxidation potential of the available trace amount of oxygen in the reaction media, i.e. oxygen dissolved or mixed in diethylene glycol during reaction.

When particle formation experiments were conducted in diethylene glycol without using acetic acid, the spherical particles were successfully formed after 10 minutes of stirring (Figure 4a). When these particles were compared to the ones fabricated using 0.25 vol% acetic acid (Figure 1a and 1b, Table 1), the particles formed without acetic acid addition were found to be much larger in size (D_{50} = 13.5 μm) indicating that the balance between the oxidation/dissolution reactions could indeed be shifted. Even though one can expect to obtain smaller particles as a result of slower oxidation reaction, without use of an acid, dissolution reactions got even much slower, and lead to formation of larger particles. Since the particle sizes are larger compared to the case where the acetic acid is used as an oxidant, the yield of undercooled particles was also relatively low (Figure 4b, Table 1). Only 24% of the fabricated particles were undercooled. The solid particles exhibited eutectic microstructure as expected.

In order to decrease the particle size, the stirring duration was increased to 22 min and 30 min. As a result, the average size (D_{50}) of the fabricated particles could be reduced to 1.7 μm and 2.3 μm, respectively (Figure 4c-f). The size of the largest particles decreased to 17.5 μm after 22 min. of stirring, and to 10.0 μm after 30 min. of stirring, indicating that the particle size distribution narrowed down with increasing stirring duration as expected. 58% of the fabricated particles were undercooled after 22 min. of stirring, whereas this ratio was increased to 97% after 30 min of stirring. As the stirring duration increased, not only the average particle size decreased, but also the undercooled particle yield at almost any size range was increased. A very small metal piece was formed when 30 min. of stirring was employed and it was useful in a way to separate the solid particles from the undercooled particles and it improved the undercooled particle yield. Therefore, it can be concluded that even the trace amount of oxygen dissolved in and/or mixed into diethylene glycol was a good enough oxidant to form BiSn liquid metal particles. Longer stirring durations with less reactive oxidant in the same reaction media balanced the shell formation reactions and enabled us to fabricate undercooled particles with high yield.

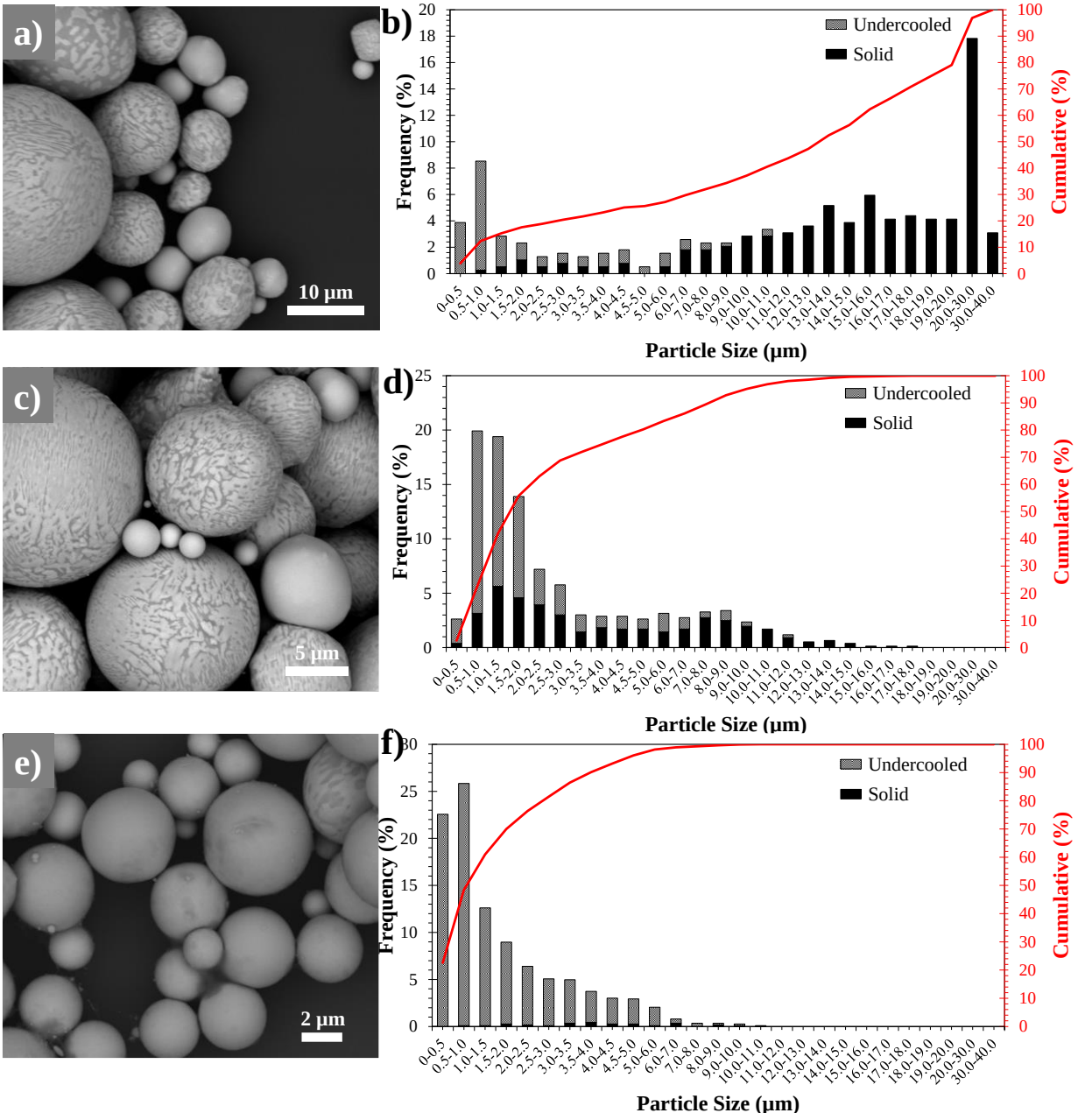

Figure 4. BSE-SEMharacterization of BiSn particles fabricated without use of acetic acid as a result of stirring for 10 min (a-b), 22 min (c-d) and 30 min (e-f). On the left side BSE-SEM micrographs were shown (a, c and d) while on the right side, contribution of the undercooled and solid particles to the particle size distribution (b, d, f) and the cumulative size distribution for total number of particles were presented.

Table 1. Particle size distribution of fabricated (both solid and undercooled) particles under various experimental conditions and the yield (the number of undercooled particles with respect to the total number of particles) of undercooled particles.

Sample	D_{10} (μm)	D_{50} (μm)	D_{90} (μm)	Yield of undercooled particles
0.25 vol% acetic acid 10 min. of stirring	0.2	2.2	6.7	80%
0.25 vol% AA 30 min. of stirring	1.2	6.8	15.3	15%
without acetic acid addition 10 min. of stirring	0.8	13.5	23.2	24%
without acetic acid addition 22 min. of stirring	0.7	1.7	8.1	58%
without acetic acid addition 30 min. of stirring	0.6	2.3	4.7	97%

3.5. The level of undercooling

In order to determine the level of undercooling, the particles fabricated with high yield were solidified using DSC. As presented in Figure 5a, the crystallization started at -8.3 °C and completed at -15 °C. The peak temperature was -12.3 °C, corresponding to the 151 degree of undercooling, which is about 0.37 T_m ($T_{m,\,BiSn} \approx 411$ K). This is one of the highest undercooling obtained for BiSn particles at eutectic composition fabricated using the droplet emulsion technique (Bogatyrenko *et al.*, 2018; Thompson and Spaepen 1983). The crystallization point of the fabricated undercooled particles were shown on the bismuth-tin phase diagram in Figure 5b.

Faster cooling rates may lead to higher undercooling. By changing the cooling rate from 1 °C /min to 20 °C /min, the peak temperature was shifted by 3 °C (Figure S1). As can be inferred from the single solidification peak in Figure 5a, the solidification temperature, thus the level of undercooling, does not change significantly in the size range of fabricated particles. The absence of the thermal event during heating proves metastability of the undercooled particles and irreversibility of the process.

Considering that the fabricated particles were washed with centrifugation at 5,000 rpm right after the particle formation process and prior to the characterization, it can be concluded that their undercooling state was stable enough under such harsh conditions. These particles could preserve their undercooled state for months under ambient conditions.

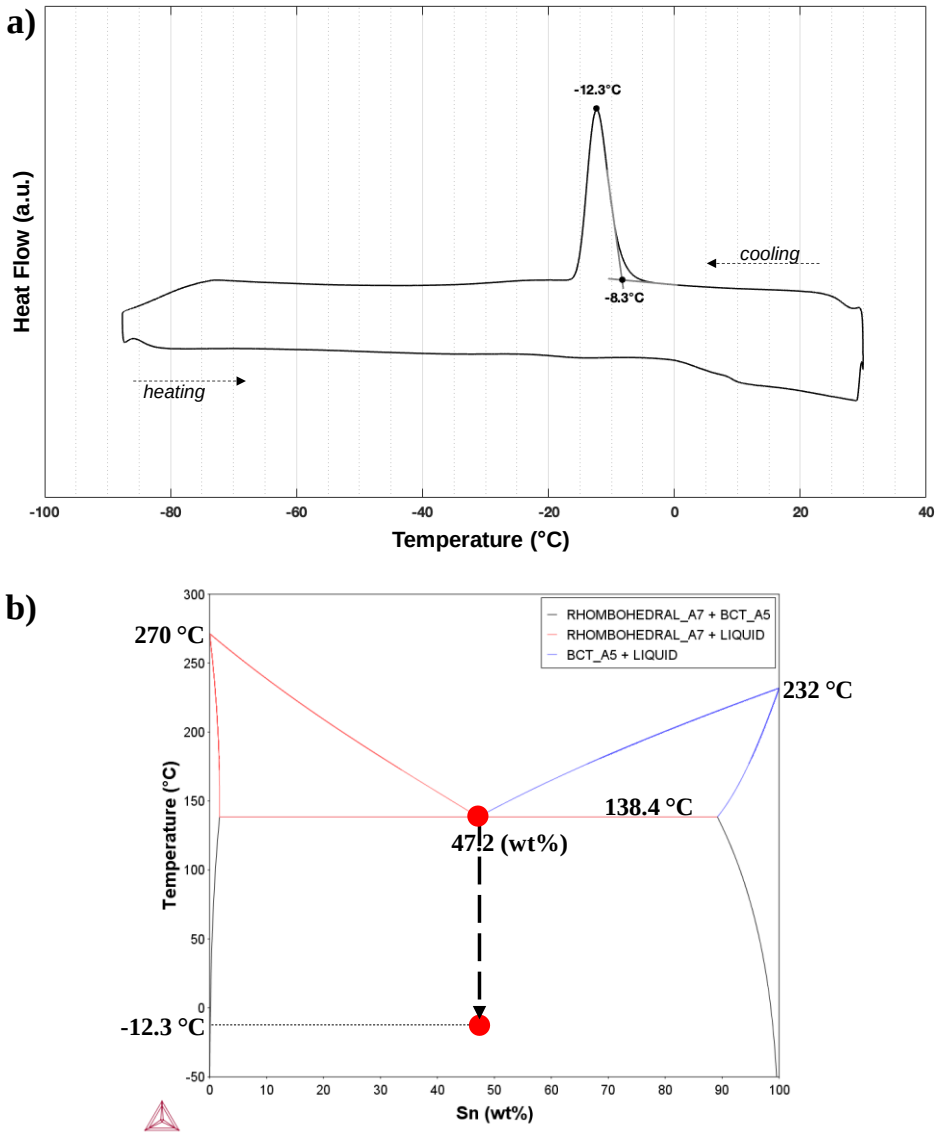

Figure 5. a) Differential scanning calorimetry analysis of the fabricated undercooled particles. The particles were fabricated by without using any oxidant and stirring for 30 min. b) The phase diagram of bismuth-tin alloy. The level of undercooling obtained for bismuth-tin particles at eutectic composition was marked on the diagram

4. CONCLUSIONS

The fabrication of the undercooled BiSn liquid metal particles at eutectic composition were studied. The size of the fabricated particles ranged from hundreds of nanometers to tens of micrometers. By increasing the stirring duration, even smaller particles could be obtained when available oxygen is used as only oxidant. Comparing the state of fabricated particles in broad size range, it was concluded that the yield of undercooled particles is higher in small sizes whereas larger particles tend to solidify more. Both acetic acid (0.25 vol% of diethylene glycol) and the available oxygen in reaction conditions are found to be good oxidants for BiSn and led to formation of spherical particles with smooth surfaces. Using the available oxygen as an oxidant allows the formation of smaller particles, thus promotes the formation of undercooled BiSn particles with high yield. The fabricated undercooled particles solidified at about -12

°C, thus the undercooling was found to be 151 °C (as high as $0.37T_m$), and can safely be used at room temperature applications. The particles can be stored for months. Based this study, it can be concluded that by the selection of the appropriate oxidant and by the optimization of processing conditions, the metastable liquid metal portfolio can be extended to other alloys with melting points higher than room temperature.

5. ACKNOWLEDGEMENTS

This study was supported by the Scientific and Technological Research Council of Turkey (TÜBİTAK) under Grant No: 117C025.

REFERENCES

Allioux, Francois-Marie, Salma Merhebi, Mohammad B Ghasemian, Jianbo Tang, Andrea Merenda, Roozbeh Abbasi, Mohannad Mayyas, et al. 2020. "Bi–Sn Catalytic Foam Governed by Nanometallurgy of Liquid Metals." *Nano Letters* 20 (6): 4403–9.

Bogatyrenko, S. I., A. A. Minenkov, and A. P. Kryshtal. 2018. "Supercooling under Crystallization of Bi-Sn Eutectic Alloy in Contact with Bi, Sn and Amorphous C." *Vacuum* 152 (June): 1–7.

Chang, Boyce S., Brijith Thomas, Jiahao Chen, Ian D. Tevis, Paul Karanja, Simge Çinar, Amrit Venkatesh, Aaron J. Rossini, and Martin M. Thuo. 2019. "Ambient Synthesis of Nanomaterials by: In Situ Heterogeneous Metal/Ligand Reactions." *Nanoscale* 11 (29): 14060–69.

Chang, Boyce S., Ravi Tutika, Joel Cutinho, Stephanie Oyola-Reynoso, Jiahao Chen, Michael D. Bartlett, and Martin M. Thuo. 2018. "Mechanically Triggered Composite Stiffness Tuning through Thermodynamic Relaxation (ST3R)." *Materials Horizons* 5 (3): 416–22.

Chen, Sen, Hong Zhang Wang, Rui Qi Zhao, Wei Rao, and Jing Liu. 2020. "Liquid Metal Composites." *Matter* 2 (6): 1446–80.

Çınar, Simge, Ian D. Tevis, Jiahao Chen, and Martin Thuo. 2016. "Mechanical Fracturing of Core-Shell Undercooled Metal Particles for Heat-Free Soldering." *Scientific Reports* 6 (1): 1–12.

Daeneke, T, K Khoshmanesh, N Mahmood, I A De Castro, D Esrafilzadeh, S J Barrow, M D Dickey, and K Kalantar-Zadeh. 2018. "Liquid Metals: Fundamentals and Applications in Chemistry." *Chem. Soc. Rev* 47: 4073.

Ding, Yu, Xuelin Guo, Yumin Qian, Leigang Xue, Andrei Dolocan, and Guihua Yu. 2020. "Room-Temperature All-Liquid-Metal Batteries Based on Fusible Alloys with Regulated Interfacial Chemistry and Wetting." *Advanced Materials*, 2002577.

Felton, Lawrence E., Christopher H. Raeder, and David B. Knorr. 1993. "The Properties of Tin-Bismuth Alloy Solders." *JOM* 45 (7): 28–32.

Firdaus, W, B Soegijono, A Sudarmadji, and A D Trisnadi. 2020. "Characterization of Bismuth in Sn-Based as Safe Environment Solder Material." *AIP Conference Proceedings* 2242: 20011.

Frongia, F., M. Pilloni, A. Scano, A. Ardu, C. Cannas, A. Musinu, G. Borzone, S. Delsante, R. Novakovic, and G. Ennas. 2015. "Synthesis and Melting Behaviour of Bi, Sn and Sn–Bi Nanostructured Alloy." *Journal of Alloys and Compounds* 623 (February): 7–14.

Gong, Mengqi, Jun Shen, Ping Nee, and Dan Hu. 2020. "Preparation of Sn-58Bi Solder Powder by Shearing Liquids into Complex Particles." *Journal of Materials Science: Materials in Electronics* 31: 5647–52.

Greer, A. Lindsay. 2010. "Materials Science: A Cloak of Liquidity." *Nature* 464 (7292): 1137–38.

Herlach, D. M., R. F. Cochrane, I. Egry, H. J. Fecht, and A. L. Greer. 1993. "Containerless Processing in the Study of Metallic Melts and Their Solidification." *International Materials Reviews* 38 (6): 273–347.

Herlach, D M. 1991. "Containerless Undercooling and Solidification of Pure Metals." *Annual Review of Materials Science* 21 (1): 23–44.

Idrus-Saidi, Shuhada A, Jianbo Tang, Jiong Yang, Jialuo Han, Torben Daeneke, Anthony P O'mullane, and Kourosh Kalantar-Zadeh. 2020. "Liquid Metal-Based Route for Synthesizing and Tuning Gas-Sensing Elements" 50: 7.

Kalantar-Zadeh, Kourosh, Jianbo Tang, Torben Daeneke, Anthony P O, Logan A Stewart, Jing Liu, Carmel Majidi, Rodney S Ruoff, Paul S Weiss, and Michael D Dickey. 2019. "Emergence of Liquid Metals in Nanotechnology." *ACS Nano* 13.

Kang, Sung K, and Amit K Sarkhel. 1994. "Lead (Pb)-Free Solders for Electronic Packaging." *Journal of Electronic Materials* 23 (8).

Kang, Yeo Kyung, Jumi Kim, Kwabena Darko, Sung Kyu Park, and Myung-Gil Kim. 2019. "Large-Scale Sonochemical Synthesis of Bi–Sn Eutectic Alloy Nanoparticles." *Journal of Nanoscience and Nanotechnology* 20 (5): 3201–5.

Kim, Hoyeon, Junyoung Lim, Jihun Kim, Jungil Lee, and Yongsok Seo. 2020. "Multilayer Structuring of Nonleaded Metal (BiSn)/Polymer/Tungsten Composites for Enhanced Γ-Ray Shielding." *Advanced Engineering Materials* 22 (6): 1901448.

Li, Hongzhe, Roozbeh Abbasi, Yifang Wang, Francois M. Allioux, Pramod Koshy, Shuhada A. Idrus-Saidi, Md Arifur Rahim, et al. 2020. "Liquid Metal-Supported Synthesis of Cupric Oxide." *Journal of Materials Chemistry C* 8 (5): 1656–65.

Lin, Yiliang, Jan Genzer, and Michael D. Dickey. 2020. "Attributes, Fabrication, and Applications of Gallium-Based Liquid Metal Particles." *Advanced Science* 7 (12): 2000192.

Liu, Nian, Guangmin Zhou, Ankun Yang, Xiaoyun Yu, Feifei Shi, Jie Sun, Jinsong Zhang, et al. 2019. "Direct Electrochemical Generation of Supercooled Sulfur Microdroplets Well below Their Melting Temperature." *Proceedings of National Academy of Science* 116 (3): 765–70.

Mahmood, Nasir, Isabela Alves De Castro, Kuppe Pramoda, Khashayar Khoshmanesh, Suresh K. Bhargava, and Kourosh Kalantar-Zadeh. 2019. "Atomically Thin Two-Dimensional Metal Oxide Nanosheets and Their Heterostructures for Energy Storage." *Energy Storage Materials* 16 (January): 455–80.

Malakooti, Mohammad H., Michael R. Bockstaller, Krzysztof Matyjaszewski, and Carmel Majidi. 2020. "Liquid Metal Nanocomposites." *Nanoscale Advances*.

Martin, Andrew, Boyce S. Chang, Zachariah Martin, Dipak Paramanik, Christophe Frankiewicz, Souvik Kundu, Ian D. Tevis, and Martin Thuo. 2019. "Heat-Free Fabrication of Metallic Interconnects for Flexible/Wearable Devices." *Advanced Functional Materials* 29 (40): 1903687.

Niu, Jiazheng, Hui Gao, Wensheng Ma, Fakui Luo, Kuibo Yin, Zhangquan Peng, and Zhonghua Zhang. 2018. "Dual Phase Enhanced Superior Electrochemical Performance of Nanoporous Bismuth-Tin Alloy Anodes for Magnesium-Ion Batteries." *Energy Storage Materials* 14 (September): 351–60.

Niu, Jiazheng, Kuibo Yin, Hui Gao, Meijia Song, Wensheng Ma, Zhangquan Peng, and Zhonghua Zhang. 2019. "Composition- and Size-Modulated Porous Bismuth-Tin Biphase Alloys as Anodes for Advanced Magnesium Ion Batteries." *Nanoscale* 11 (32): 15279–88.

Perepezko, J. H., and J. S. Paik. 1981. "Undercooling Behavior of Liquid Metals." In *MRS Proceedings*, 8:49. Cambridge University Press.

Perepezko, J. H., and G. Wilde. 2016. "Melt Undercooling and Nucleation Kinetics." *Current Opinion in Solid State and Materials Science* 20 (1): 3–12.

Perepezko, John H. 1984. "Nucleation in Undercooled Liquids." *Materials Science and Engineering* 65 (1): 125–35.

Qu, Ke, Hong Zhang, Qianqian Lan, Xia Deng, Xinlong Ma, Yuanqing Huang, Junwei Zhang, et al. 2015. "Realization of the Welding of Individual TiO2 Semiconductor Nano-Objects Using a Novel 1D Au80Sn20 Nanosolder." *Journal of Materials Chemistry C* 3 (43): 11311–17.

Rasmussen, Don H., and Jr. Carl R. Loper. 1975. Micron sized spherical droplets of metals and method. US4042374A, issued March 20, 1975.

Schülli, T U, R Daudin, G Renaud, A Vaysset, O Geaymond, and & A Pasturel. 2010. "Substrate-Enhanced Supercooling in AuSi Eutectic Droplets." *Nature* 464.

Silva, Cristian A., Jian Lv, Lu Yin, Itthipon Jeerapan, Gabriel Innocenzi, Fernando Soto, Young-Geun Ha, and Joseph Wang. 2020. "Liquid Metal Based Island-Bridge Architectures for All Printed Stretchable Electrochemical Devices." *Advanced Functional Materials*, 2002041.

Tevis, I. D., Newcomb, L. B., Thuo, M. 2014. "Synthesis of Liquid Core-Shell Particles and Solids Patchy Multicomponent Particles by Shearing Liquids Into Complex Particles (SLICE)." *Langmuir* 30 (47): 14308-13.

Thompson, C. V., and F. Spaepen. 1983. "Homogeneous Crystal Nucleation in Binary Metallic Melts." *Acta Metallurgica* 31 (12): 2021–27.

Wang, Lei, and Jing Liu. 2013. "Liquid Metal Material Genome: Initiation of a New Research Track towards Discovery of Advanced Energy Materials." *Frontiers in Energy* 7 (3): 317–32.

Wang, Qian, Yang Yu, and Jing Liu. 2018a. "Preparations, Characteristics and Applications of the Functional Liquid Metal Materials." *Advanced Engineering Materials* 20 (5): 1700781.

Wang, Xuelin, Rui Guo, and Jing Liu. 2018b. "Liquid Metal Based Soft Robotics: Materials, Designs, and Applications." *Advanced Materials Technologies* 4 (2): 1800549.

Xu, Chengtao, Biao Ma, Shuai Yuan, Chao Zhao, and Hong Liu. 2020. "High-Resolution Patterning of Liquid Metal on Hydrogel for Flexible, Stretchable, and Self-Healing Electronics." *Advanced Electronic Materials* 6 (1): 1900721.

Yuan, Tingbiao, Zheng Hu, Yuxin Zhao, Jinjie Fang, Jun Lv, Qinghua Zhang, Zhongbin Zhuang, Lin Gu, and Shi Hu. 2020. "Two-Dimensional Amorphous SnO x from Liquid Metal: Mass Production, Phase Transfer, and Electrocatalytic CO 2 Reduction toward Formic Acid." *Nano Letters* 20: 2916–22.

Zahir, Md Hasan, Shamseldin A. Mohamed, R. Saidur, and Fahad A. Al-Sulaiman. 2019. "Supercooling of Phase-Change Materials and the Techniques Used to Mitigate the Phenomenon." *Applied Energy* 240 (April): 793–817.

Zhai, Q.J., Y.L. Gao, W.B. Guan, and K.D. Xu. 2006. "Role of Size and Cooling Rate in Quenched Droplet of SnBi Eutectic Alloy." *Materials Science and Engineering: A* 441 (1–2): 278–81.

Supporting Information

FABRICATION OF UNDERCOOLED BISMUTH TIN LIQUID METAL PARTICLES WITH HIGH YIELD

Simge Çınar[1,*]

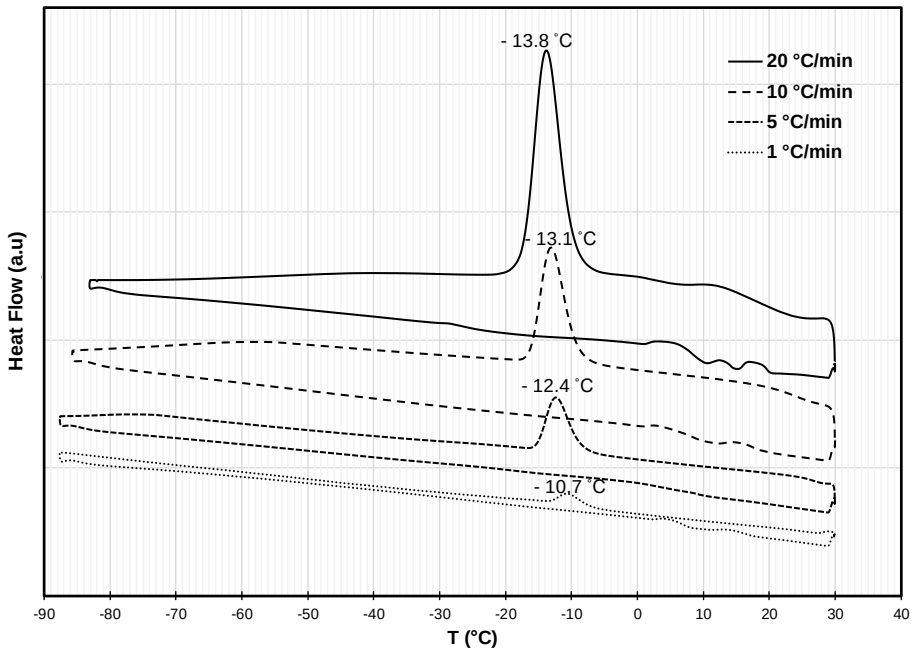

Figure S1. The effect of cooling rate on the solidification temperature of undercooled BiSn micro-/nano-particles. The peak temperatures of crystallization were found to be -11 °C, -12 °C, -13 °C and -14 °C when the samples were cooled with the rates of 1 °C/min, 5 °C/min, 10 °C/min and 20 °C/min, respectively.